Journal of Global Change Data & Discovery. 2022, 6(3): 479-486
www.geodoi.ac.cn

Methodology of 0.625°×0.4712° Raster Dataset Development of Temperature at the Top of Permafrost and Active Layer Thickness in the Northern Hemisphere (2015–2100)

Wu, X. R.[1, 2] Zhao, N.[1, 2, 3*] Ye, Y. L.[4]

1. State Key Laboratory of Resources and Environmental Information System, Institute of Geographic Sciences and Natural Resources Research, Chinese Academy of Sciences, Beijing 100101, China;
2. College of Resources and Environment, University of Chinese Academy of Sciences, Beijing 100049, China;
3. Jiangsu Center for Collaborative Innovation in Geographic Information Resource Development and Application, Nanjing 210023, China;
4. Zhengyuan Geomatics Group Co., Ltd., Beijing 101300, China

Abstract: Understanding the spatial distribution and dynamics of current and future permafrost is critical for global carbon flow simulation, climate change prediction, and engineering risk assessment. The 0.625°x0.4712° raster dataset of temperature at the top of permafrost and active layer thickness in the northern hemisphere (2015–2100) was developed using the widely validated and applied Kudryavtsev method, which integrates the effects of temperature, snow, vegetation, and soil on permafrost, based on the model outputs from the sixth phase of the International Coupled Model Intercomparison Project (CMIP6) and the SoilGrids 2.0 dataset. The data were calculated under four different scenarios, SSP126, SSP245, SSP370, and SSP585, from 2015 to 2100. The permafrost area was obtained based on the temperature at the top of the permafrost. This dataset fills the gap in permafrost distribution data for the future under different scenarios for CMIP6. It includes the data covering 2015–2100: (1) mean annual temperature at the top of the permafrost; (2) annual active layer thickness; and (3) annual permafrost area. The resolution of the spatial data is 0.625°x0.4712°. The dataset is archived in .tif and .xls data formats, and consists of 690 data files with data size of 35.6 MB (Compressed to one single file with 27.9 MB).

Keywords: permafrost; temperature at the top of permafrost; active layer thickness; Kudryavtsev; CMIP6; northern hemisphere; Prediction

DOI: https://doi.org/10.3974/geodp.2022.03.19

CSTR: https://cstr.escience.org.cn/CSTR:20146.14.2022.03.19

Received: 20-07-2022; **Accepted:** 17-09-2022; **Published:** 25-09-2022

Foundation: Chinese Academy of Sciences (XDA20030203)

***Corresponding Author:** Zhao, N., Institute of Geographic Sciences and Natural Resources Research, Chinese Academy of Sciences, zhaon@lreis.ac.cn

Data Citation: [1] Wu, X. R., Zhao, N., Ye, Y. L. Methodology of 0.625°×0.4712° raster dataset development of temperature at the top of permafrost and active layer thickness in the northern hemisphere (2015–2100) [J]. *Journal of Global Change Data & Discovery*, 2022, 6(3): 479–486. https://doi.org/10.3974/geodp.2022.03.19. https://cstr.escience.org.cn/CSTR:20146. 14.2022.03.19.

[2] Wu, X. R., Zhao, N. 0.625°×0.4712° raster dataset of temperature at the top of permafrost and active layer thickness in the northern hemisphere (2015–2100) [J/DB/OL]. *Digital Journal of Global Change Data Repository*, 2022. https://doi.org/10.3974/geodb.2022.08.01.V1. https://cstr.escience.org.cn/CSTR:20146.11.2022.08.01.V1.

Dataset Availability Statement:

The dataset supporting this paper was published and is accessible through the *Digital Journal of Global Change Data Repository* at: https://doi.org/10.3974/geodb.2022.08.01.V1 or https://cstr.escience.org.cn/CSTR:20146.11.2022.08.01.V1.

1 Introduction

Permafrost is ground with temperatures below 0 °C that has been frozen for at least two consecutive years[1], occupies approximately 25% of the global land surface[2] and affects most northern hemisphere regions to varying degrees[3]. Closely linked to several domains, such as the atmosphere, hydrosphere, and lithosphere, permafrost is highly susceptible to environmental influences and has significant feedbacks on other domains. In the last decades, shrinking permafrost areas and increasing active layer thickness have become increasingly prominent due to global warming[4]. The degradation of permafrost has caused a series of complex and serious consequences. For example, the change of permafrost to seasonally frozen ground increases the emissions of organic carbon and methane in the soil, further contributing to global warming[5]. In addition, the degradation of permafrost changes the physical and chemical properties of the surface and subsurface in the local and surrounding areas, posing a serious safety risk to infrastructure and engineering projects[6]. Furthermore, warming of permafrost-influenced soil has a direct impact on Arctic ecosystems[6]. Therefore, evaluating the spatial distribution and dynamics of current and future permafrost is essential for global carbon flow simulation, climate change prediction, and engineering risk assessment[2].

Several studies have been conducted to estimate the future distribution of permafrost and active layer thickness using empirical formulas or physical models[2, 7–9]. However, most of them have not published the corresponding datasets, which has somewhat delayed the launch of subsequent studies. In terms of the data chosen, no studies have used the sixth phase of the International Coupled Model Intercomparison Project (CMIP6) model outputs as climate input to develop data on the future dynamics of permafrost in the northern hemisphere, while the near-surface air temperature and snow thickness available in the CMIP6 have been shown to be the most important factors influencing permafrost models[10]. In addition, most previous studies have been conducted over a period of more than ten or several decades, and this temporal resolution does not meet the needs of studies with shorter study periods. Researchers have also been unable to obtain the average state or series of permafrost data for their own study period. The semi-empirical and semi-theoretical Kudryavtsev method has been shown to be more effective and widely used for calculating permafrost active layer thickness under different climatic conditions[10–13] and is suitable for large-scale applications in the northern hemisphere.

In this study, the Kudryavtsev method was applied, using the model outputs from CMIP6 (CMCC-CM2-SR5[14] and CMCC-ESM2[15]) and SoilGrids 2.0[16] soil data, to calculate the time series of the temperature at the top of permafrost and active layer thickness in permafrost areas on a yearly scale in the northern hemisphere. This dataset fills the gap in permafrost data for the future under different scenarios for CMIP6 and provides data support for research related to permafrost degradation, climate change, and Arctic ecology.

2 Metadata of the Dataset

The metadata of the 0.625°×0.4712° raster dataset of temperature at the top of permafrost and active layer thickness in the northern hemisphere (2015–2100)[17] is summarized in Table 1. It includes the dataset full name, short name, authors, year of the dataset, temporal resolution, spatial resolution, data format, data size, data files, data publisher, and data shar-

ing policy, etc.

Table 1 Metadata summary of the 0.625°×0.4712° raster dataset of temperature at the top of permafrost and active layer thickness in the northern hemisphere (2015–2100)

Items	Description
Dataset full name	0.625°×0.4712° raster dataset of temperature at the top of permafrost and active layer thickness in the northern hemisphere (2015–2100)
Dataset short name	NH_Permafrost_2015-2100
Authors	Wu, X. R., Institute of Geographic Sciences and Natural Resources Research, Chinese Academy of Sciences, wu_xiaoran@outlook.com Zhao, N., Institute of Geographic Sciences and Natural Resources Research, Chinese Academy of Sciences, zhaon@lreis.ac.cn
Geographical region	Northern hemisphere
Year	2015–2100
Temporal resolution	Yearly
Spatial resolution	0.625°×0.4712°
Data format	.tif, .xls
Data size	35.6 MB
Data files	(1) mean annual temperature at the top of permafrost; (2) annual active layer thickness; and (3) annual permafrost area
Foundation	Chinese Academy of Sciences (XDA20030203)
Computing environment	Microsoft 365, ArcGIS, R
Data publisher	Global Change Research Data Publishing & Repository, http://www.geodoi.ac.cn
Address	No. 11A, Datun Road, Chaoyang District, Beijing 100101, China
Data sharing policy	***Data*** from the Global Change Research Data Publishing & Repository includes metadata, datasets (in the *Digital Journal of Global Change Data Repository*), and publications (in the *Journal of Global Change Data & Discovery*). ***Data*** sharing policy includes: (1) ***Data*** are openly available and can be free downloaded via the Internet; (2) End users are encouraged to use ***Data*** subject to citation; (3) Users, who are by definition also value-added service providers, are welcome to redistribute ***Data*** subject to written permission from the GCdataPR Editorial Office and the issuance of a ***Data*** redistribution license; and (4) If ***Data*** are used to compile new datasets, the 'ten per cent principal' should be followed such that ***Data*** records utilized should not surpass 10% of the new dataset contents, while sources should be clearly noted in suitable places in the new dataset[18]
Communication and searchable system	DOI, CSTR, Crossref, DCI, CSCD, CNKI, SciEngine, WDS/ISC, GEOSS

3 Methods

3.1 Data Collection

CMIP6 has the largest number of models involved, the most well-designed scientific experiments, and the largest amount of simulation data available in the more than 20 years of the CMIP program[19]. It uses a combined matrix of shared socio-economic pathways (SSPs, representing different development patterns of future economic and social systems) and representative concentration pathways (RCPs, representing target radiative forcing values for the end of the 21st century) to form different scenarios for the future. Scenario SSP126 is a combination of scenario SSP1 (sustainability) and scenario RCP2.6. Scenario SSP245 is a combination of scenario SSP2 (middle of the road) and scenario RCP4.5. Scenario SSP370 is a combination of scenario SSP3 (regional rivalry) and scenario RCP7.0. Scenario SSP585 is a combination of scenario SSP5 (fossil-fuelled development) and scenario RCP8.5.

In this study, near-surface air temperature (tas), snow thickness (snd) and soil moisture (mrso) from two models, CMCC-CM2-SR5[14] and CMCC-ESM2[15], were selected based on temporal resolution, spatial resolution and experiment-driven conditions. These variables span the 2015–2100 period with a global spatial resolution of 288×192 pixels and have out-

puts under four typical scenarios (SSP126, SSP245, SSP370 and SSP585).

The SoilGrids 2.0 dataset[16] uses state-of-the-art machine learning methods to map the global spatial distribution of soil properties with a spatial resolution of 250 m and contains six standard depth intervals (0–5 cm, 5–15 cm, 15–30 cm, 30–60 cm, 60–100 cm and 100–200 cm). Five parameters from SoilGrids 2.0 were selected in this study: clay content, t sand content, silt content, soil organic matter content and soil bulk density. Soil data from six intervals were weighted and averaged and resampled to a spatial resolution of 0.625°×0.4712°.

3.2 Kudryavtsev Method

The Kudryavtsev method is a widely used and validated semi-empirical approach that integrates the effects of snow, vegetation, soil moisture, soil thermal properties and other factors on the active layer. It divides the complex atmosphere-permafrost system into separate components and considers the thermal conditions of the components individually[20]. The main calculations are as follows[1, 2, 8, 10, 21].

The Kudryavtsev method assumes that the annual variation in air temperature can be approximated as a cosine function. Then, the temperature $T(t)$ can be expressed as:

$$T(t) = T_a + A_a \cdot \cos(2\pi \cdot t / P) \tag{1}$$

where T_a and A_a are the annual mean air temperature and the annual mean air temperature amplitude, respectively. t is time, and P is the period of temperature change (1 year).

The surface temperature can be considered the result of the effect of air temperature through snow and vegetation; therefore, the annual mean surface temperature (T_s) and the annual mean surface temperature amplitude (A_s) can be expressed as:

$$T_s = T_a + \Delta T_{sn} + \Delta T_{veg} \tag{2}$$

$$A_s = A_a - \Delta A_{sn} - \Delta A_{veg} \tag{3}$$

where ΔT_{sn} and ΔA_{sn} are the snow cover effects on the mean annual air temperature and the seasonal amplitude, respectively. Similarly, ΔT_{veg} and ΔA_{veg} are the vegetation effects on the mean annual air temperature and the seasonal amplitude, respectively.

$$\Delta T_{sn} = \Delta A_{sn} = A_a \cdot \left\{ 1 - \exp \cdot \left[-Z_{sn} \cdot \left(\frac{\pi}{P \cdot K_{sn}} \right)^{1/2} \right] \right\} \tag{4}$$

$$\Delta T_{veg} = \frac{\Delta A_1 \cdot \tau_1 - \Delta A_2 \cdot \tau_2}{P} \cdot \frac{\pi}{2} \tag{5}$$

$$\Delta A_{veg} = \frac{\Delta A_1 \cdot \tau_1 + \Delta A_2 \cdot \tau_2}{P} \tag{6}$$

$$\Delta A_1 = \left(A_{veg} - T_{veg} \right) \cdot \left\{ 1 - \exp \left[-Z_{veg}^f \cdot \left(\frac{\pi}{K_{veg}^f \cdot 2\tau_1} \right)^{1/2} \right] \right\} \tag{7}$$

$$\Delta A_2 = \left(A_{veg} + T_{veg} \right) \cdot \left\{ 1 - \exp \left[-Z_{veg}^t \cdot \left(\frac{\pi}{K_{veg}^t \cdot 2\tau_2} \right)^{1/2} \right] \right\} \tag{8}$$

$$A_{veg} = A_a - \Delta A_{sn} \tag{9}$$

$$T_{veg} = T_a + \Delta T_{sn} \tag{10}$$

where Z_{sn} and K_{sn} are the thickness and the thermal diffusion coefficient of snow, respectively. τ_1 and τ_2 are the durations of the cold and warm periods, respectively. $Z_{vegt/f}$ and $K_{vegt/f}$ are the thickness and the thermal diffusion coefficient of the vegetation in the thawed/

freezing state, respectively.

Finally, the mean annual temperature at the depth of seasonal thaw (T_z), i.e., the temperature at the top of the permafrost, can be expressed as:

$$T_{numerator} = 0.5T_s \cdot \left(\lambda_f + \lambda_t\right) + A_s \cdot \frac{\lambda_t - \lambda_f}{\pi} \cdot \left[\frac{T_s}{A_s} \cdot \arcsin\left(\frac{T_s}{A_s}\right) + \left(1 - \frac{T_s^2}{A_s^2}\right)^{1/2} \right. \tag{11}$$

$$T_z = \frac{T_{numerator}}{\lambda^*}, \lambda^* = \begin{cases} \lambda_f, if\ T_{numerator} < 0 \\ \lambda_t, if\ T_{numerator} > 0 \end{cases} \tag{12}$$

where $\lambda_{t/f}$ is the thermal conductivity of the soil in the thawed/freezing state.

The active layer thickness (Z) is calculated as:

$$Z = \frac{2\left(A_s - T_z\right) \cdot \left(\frac{\lambda \cdot P \cdot C}{\pi}\right)^{\frac{1}{2}} + \frac{\left(2A_z \cdot C \cdot Z_c + Q_{ph} \cdot Z_c\right) \cdot Q_{ph} \cdot \left(\frac{\lambda \cdot P}{\pi \cdot C}\right)^{1/2}}{2A_z \cdot C \cdot Z_c + Q_{ph} \cdot Z_c + \left(2A_z \cdot C + Q_{ph}\right) \cdot \left(\frac{\lambda \cdot P}{\pi \cdot C}\right)^{1/2}}}{2A_z \cdot C + Q_{ph}} \tag{13}$$

$$A_z = \frac{A_s - T_z}{\ln\left(\frac{A_s + Q_{ph}/2C}{|T_z| + Q_{ph}/2C}\right)} - \frac{Q_{ph}}{2C} \tag{14}$$

$$Z_c = \frac{2\left(A_s - T_z\right) \cdot \sqrt{\frac{\lambda_t \cdot P \cdot C}{\pi}}}{2A_z \cdot C + Q_{ph}} \tag{15}$$

$$\lambda, C = \begin{cases} \lambda_f, C_f, if\ T_z < 0 \\ \lambda_t, C_t, fi\ T_z > 0 \end{cases} \tag{16}$$

where $C_{t/f}$ is the volumetric heat capacity of the soil in the thawed/frozen state and Q_{ph} is the phase transition heat in the active layer.

4 Data Results and Validation

4.1 Data Composition

The ActiveLayerThickness folder contains active layer thickness data in 344 files. The Temperature folder contains temperature at the top of the permafrost data in 344 files. File "NH_PermafrostArea.xls" is the permafrost area time series data in km^2. The "ReadMe.txt" is the instructions file.

4.2 Data Products

As shown in Figure 1, the permafrost in the northern hemisphere is mainly distributed in three regions, the mid and high latitudes of northeastern Eurasia, the high latitudes of the northern North American continent and the Tibetan Plateau, in decreasing order of area. In the first two regions, the active layer thickness decreases from south to north, while the thinnest active layers in the Tibetan Plateau region are in the western and central-northern regions.

The distribution of permafrost degradation is similar across the four scenarios for the 2015–2050 period. It is mainly found in the southwestern Eurasian permafrost region and in

the southern North American continental permafrost region. The northwestern Qinghai-Tibet Plateau region shows a smaller decrease in permafrost area, while the change in active layer thickness increases with increasing latitude.

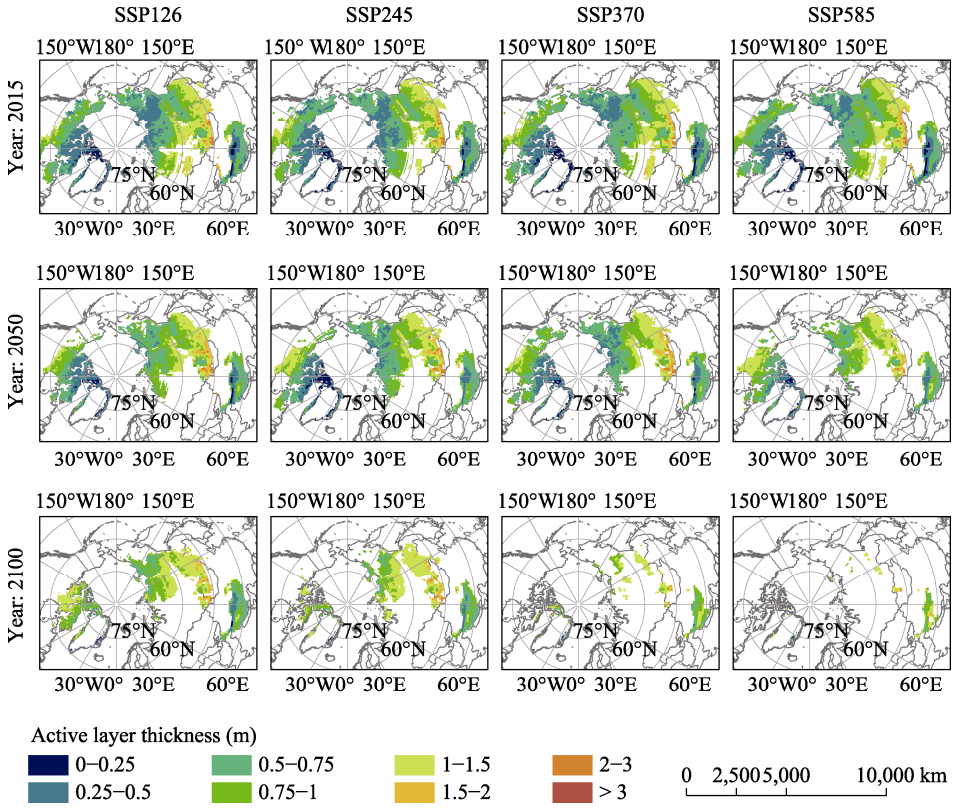

Figure 1 Active layer thickness in the northern hemisphere under different scenarios in 2015, 2050 and 2100

Between 2050 and 2100, the differences in permafrost degradation between the scenarios are highly significant. (1) Scenario SSP126: relatively little area of permafrost loss and a small increase in active layer thickness, mainly in the northern North American continental permafrost region and the eastern Eurasian permafrost region. (2) Scenario SSP245: significant decrease in permafrost area in the southern North American continental and Eurasian permafrost regions, with a rapid increase in active layer thickness in the northernmost North American continental permafrost regions. (3) Scenario SSP370: significant reduction in permafrost area in the northern hemisphere, with near disappearance of permafrost in the northern North American continent permafrost region and severe degradation of permafrost in the Eurasian and Qinghai-Tibet Plateau permafrost regions. (4): Scenario SSP585: near disappearance of permafrost area in the northern hemisphere, significant increase in active layer thickness in the remaining permafrost regions and severe permafrost degradation on the Qinghai-Tibet Plateau.

As shown in Figure 2, the northern hemisphere permafrost area in 2015 was approximately 20.99×10^6 km^2 (estimated under scenario SSP245). In addition, the northern hemisphere permafrost area shows a fluctuating decreasing trend under all four scenarios: SSP126, SSP245, SSP370 and SSP585. Specifically, the end-of-century permafrost areas under the four scenarios are 10.62×10^6 km^2, 8.48×10^6 km^2, 3.13×10^6 km^2 and 1.34×10^6 km^2, which represent decreases of 49.37%, 59.60%, 85.09% and 93.63%, respectively, compared to 2015.

4.3 Data Validation

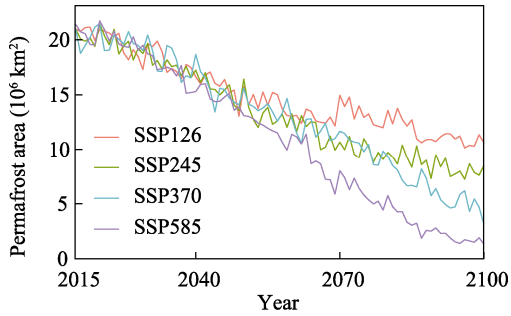

Figure 2 Time series of the northern hemisphere permafrost area under different scenarios (2015–2100)

CMIP6 provides model outputs under different scenarios from 2015 to 2100; therefore, there are no corresponding ground observations that can be used as validation data. Generally, the way to assess the accuracy of time series prediction models is to validate the historical record. Numerous studies using the Kudryavtsev method have been conducted in different regions[1, 10–13, 20–22] and they concluded that this model is able to simulate the permafrost distribution and active layer thickness well. Among the model input data in this study, the model outputs of CMIP6 are currently the most authoritative and applied data for predicting environmental variables under different scenarios[19], while SoilGrids 2.0 is a widely used high-precision soil dataset[16].

The area of permafrost in the northern hemisphere estimated in this study was approximately 20.99×10^6 km^2 in 2015, compared to 21.64×10^6 km^2 (2014–2018)[2], 22.79×10^6 km^2 (1920s–1990s)[23] and 19.96×10^6 km^2 (2000–2015, without considering vegetation effects)[24]. Therefore, the estimates of permafrost area in the northern hemisphere in this study can be considered reasonable.

5 Discussion and Conclusion

The accuracy of the Kudryavtsev method has been well validated in historical records. However, some model inputs, such as vegetation properties and soil texture, are often set to constant values due to their unavailability under different future scenarios, which affects the model accuracy. In addition, near-surface air temperature and snow thickness are the most critical factors in the permafrost model, but the coarse resolution of the CMIP6 model outputs leads to the coarse resolution of the produced dataset. This makes it difficult and uncertain to directly apply the dataset to local studies with large spatial heterogeneity.

Shrinking the permafrost area and increasing the active layer thickness will result in serious climate feedbacks, ecological problems and engineering risks, while global climate change has been accelerating permafrost degradation. Their interactions may cause more complex and unpredictable changes to the climate, ecology and other environments in the future. Predicting the future development of permafrost will help to understand the response of permafrost to global climate change and to prepare for possible ecological and engineering problems. Given the lack of predictive data of future northern hemisphere permafrost, this study developed a time series of permafrost data under different scenarios using the Kudryavtsev method, which has been shown to perform well, with the CMIP6 model outputs and SoilGrids dataset as input. The dataset provides predictions of the spatial distribution, active layer thickness and area changes of permafrost for up to 86 years, providing data support for research related to permafrost degradation, climate change and Arctic ecology.

Author Contributions

Zhao, N. was primarily responsible for the dataset design and reviewed the data paper; Wu, X. R. collected and processed data such as soil and climate and wrote the data paper; Ye, Y. L. optimized the model algorithm and reviewed the data paper.

Conflicts of Interest

The authors declare no conflicts of interest.

References

[1] Shiklomanov, N. I., Nelson, F. E. Analytic representation of the active layer thickness field, Kuparuk River Basin, Alaska [J]. *Ecological Modelling*, 1999, 123(2/3): 105–125.

[2] Li, G. J., Zhang, M. Y., Pei, W. S., *et al*. Changes in permafrost extent and active layer thickness in the Northern Hemisphere from 1969 to 2018 [J]. *Science of the Total Environment*, 2022, 804: 150182.

[3] Zhang, T., Barry, R., Knowles, K., *et al*. Statistics and characteristics of permafrost and ground-ice distribution in the northern hemisphere [J]. *Polar Geography*, 2008, 31(1/2): 47–68.

[4] Streletskiy, D. Permafrost degradation [C]. In: Haeberli, W., Whiteman, C. (eds). Snow and Ice-Related Hazards, Risks, and Disasters (Second Edition). Amsterdam: Elsevier, 2021: 297–322. https://doi.org/10.1016/B978-0-12-817129-5.00021-4.

[5] Moon, T. A., Overeem, I., Druckenmiller, M., *et al*. The Expanding Footprint of Rapid Arctic Change [J]. *Earth's Future*, 2019, 7(3): 212–218.

[6] Melvin, A. M., Larsen, P., Boehlert, B., *et al*. Climate change damages to Alaska public infrastructure and the economics of proactive adaptation [J]. *Proceedings of the National Academy of Sciences*, 2017, 114(2): E122–E131.

[7] Wu, Q. B., Li, X., Li, W. J. The prediction of permafrost change along the Qinghai-Tibet Highway, China [J]. *Permafrost and Periglacial Processes*, 2000, 11(4): 371–376.

[8] Liu, L., Zhao, D. S., Wei, J. Q., *et al*. Permafrost sensitivity to global warming of 1.5 degrees C and 2 degrees C in the northern hemisphere [J]. *Environmental Research Letters*, 2021, 16(3): 034038.

[9] Zhao, S. M., Cheng, W. M., Yuan, Y. C., *et al*. Global permafrost simulation and prediction from 2010 to 2100 under different climate scenarios [J]. *Environmental Modelling & Software*, 2022, 149: 105307.

[10] Wang, K., Jafarov, E., Overeem, I. Sensitivity evaluation of the Kudryavtsev permafrost model [J]. *Science of the Total Environment*, 2020, 720: 137538.

[11] Panda, S., Romanovsky, V., Marchenko, S. High-resolution permafrost modeling in the Arctic Network National Parks, Preserves and Monuments [R]. Colorado: National Park Service, 2016. https://irma.nps.gov/DataStore/Reference/Profile/2237720.

[12] Streletskiy, D. A., Shiklomanov, N. I., Nelson, F. E. Spatial variability of permafrost active-layer thickness under contemporary and projected climate in Northern Alaska [J]. *Polar Geography*, 2012, 35(2): 95–116.

[13] Sazonova, T. S., Romanovsky, V. E. A model for regional-scale estimation of temporal and spatial variability of active layer thickness and mean annual ground temperatures [J]. *Permafrost and Periglacial Processes*, 2003, 14(2): 125–39.

[14] Lovato, T., Peano, D. CMCC CMCC-CM2-SR5 model output prepared for CMIP6 ScenarioMIP. Version 20200622 [DS]. Earth System Grid Federation, 2020. https://doi.org/10.22033/ESGF/CMIP6.1365.

[15] Lovato, T., Peano, D., Butenschön, M. CMCC CMCC-ESM2 model output prepared for CMIP6 ScenarioMIP. Version 20210202 [DS]. Earth System Grid Federation, 2021. https://doi.org/10.22033/ESGF/CMIP6.13168.

[16] Poggio, L., De Sousa, L. M., Batjes, N. H., *et al*. SoilGrids 2.0: producing soil information for the globe with quantified spatial uncertainty [J]. *Soil*, 2021, 7(1): 217–240.

[17] Wu, X. R., Zhao, N. 0.625°×0.4712° raster dataset of temperature at the top of permafrost and active layer thickness in the northern hemisphere (2015–2100) [J/DB/OL]. *Digital Journal of Global Change Data Repository*, 2022. https://doi.org/10.3974/geodb.2022.08.01.V1. https://cstr.escience.org.cn/CSTR:20146.11.2022.08.01.V1.

[18] GCdataPR Editorial Office. GCdataPR data sharing policy [OL]. https://doi.org/10.3974/dp.policy.2014.05 (Updated 2017).

[19] Eyring, V., Bony, S., Meehl, G. A., *et al*. Overview of the Coupled Model Intercomparison Project Phase 6 (CMIP6) experimental design and organization [J]. *Geoscientific Model Development*, 2016, 9(5): 1937–1958.

[20] Wang, C. H., Jin, S. L., Wu, Z. Y., *et al*. Evaluation and application of the estimation methods of frozen (thawing) depth over China [J]. *Advances in Earth Science*, 2009, 24(2):132–140.

[21] Anisimov, O. A., Shiklomanov, N. I., Nelson, F. E. Global warming and active-layer thickness: results from transient general circulation models [J]. *Global and Planetary Change*, 1997, 15(3/4): 61–77.

[22] Wang, C. H., Jin, S. L., Shi, H. X. Area change of the frozen ground in China in the next 50 years [J]. *Journal of Glaciology and Geocryology*, 2014, 36(1): 1–8.

[23] Zhang, T., Heginbottom, J. A., Barry, R. G., *et al*. Further statistics on the distribution of permafrost and ground ice in the northern hemisphere [J]. *Polar Geography*, 2000, 24(2): 126–131.

[24] Shi, Y. Y., Niu, F. J., Lin, Z. J., *et al*. Freezing/thawing index variations over the circum-Arctic from 1901 to 2015 and the permafrost extent [J]. *Science of the Total Environment*, 2019, 660: 1294–1305.